J. Fluid Mech. (1993), *vol.* 255, *pp.* 647–665

The effect of applied pressure on the shape of a two-dimensional liquid curtain falling under the influence of gravity

By DOUGLAS S. FINNICUM, STEVEN J. WEINSTEIN AND KENNETH J. RUSCHAK

Emulsion Coating Technologies, Eastman Kodak Company, Rochester, NY 14652–3701, USA

(Received 19 May 1992 and in revised form 23 March 1993)

The shape of a two-dimensional liquid curtain issuing from a slot and falling under the influence of gravity is predicted theoretically and verified experimentally for cases where a pressure is applied to the curtain. A set of approximate equations is derived which governs the location of the curtain for a liquid having surface tension σ, density ρ, volumetric flow per unit width Q, and local free-fall velocity V. These equations possess a singularity at the point where the local Weber number, $We = \rho QV/2\sigma$, is equal to 1. Despite the fact that previous work on the stability of two-dimensional curtains shows that curtains having locations where $We < 1$ are unstable to small disturbances, our experiments show that these curtains can exist over a wide range of flow conditions. Thus, it is necessary to consider how the singularity is resolved when a pressure is applied.

It is found that the singularity can be eliminated from the governing equations if the curtain assumes a definite direction as it leaves the slot. By contrast, if the curtain leaves the slot such that $We > 1$, there is no such restriction, and experimentally it is found that the curtain leaves parallel to the slot walls. The theoretical predictions of the curtain shapes are in agreement with those measured experimentally for all Weber numbers investigated.

1. Introduction

Liquid sheets are found in a wide variety of physical configurations and are thus a subject of industrial and academic interest. Two-dimensional liquid sheets falling under the influence of gravity are employed to deposit a thin, uniform film on a moving solid substrate during coating processes. Annular liquid sheets are used to protect the inner walls of laser fusion reactors and to aid in the direct reduction of certain metals. The spinning and extensional rheological measurement of polymer fibres can be achieved in configurations employing two-dimensional sheets. Water bells, the axisymmetric sheets of liquid formed by impingement on a solid surface, can achieve a wide variety of fascinating shapes with seemingly small changes in flow and ambient conditions.

Much of the work examining the shapes and stability of liquid sheets has been done in the context of water bells. The sensitivity of the shapes of liquid sheets to ambient conditions was demonstrated by Hopwood (1952), who showed that a small pressure difference across a water bell could radically change the shape of the bell. Lance & Perry (1953) further experimentally investigated the effects of pressure and theoretically derived the differential equations governing the shape of water bells by modifying the

equations of Boussinesq (1869*a*, *b*). Lance & Perry's equations assumed that the shape of a water bell was described by the location of the centreline of the liquid sheet about which the thickness of the sheet varied slowly. Furthermore, the effects of the external air drag and the fluid viscosity were neglected, and plug flow was assumed locally; such assumptions led directly to a free-fall velocity in the liquid. Although Lance & Perry's experimental and theoretical shapes were in good agreement, the comparisons were not absolute because they could not satisfactorily measure the small pressure difference across the bell. In a related problem governed by the same equations as for water bells, Ramos (1988) has theoretically demonstrated that a very small pressure difference across a liquid annular sheet can dramatically increase the length of the annular sheet beyond which it closes and becomes a cylindrical jet of liquid (convergence length).

The equations of Lance & Perry (1953) are clearly not valid in the vicinity of the entrance region where the bell is created, since the flow is not of plug type there; the bell must adjust to the change in boundary conditions where it originates, and this effect is not accounted for by the water bell equations. An analogous entrance effect is seen when a two-dimensional liquid sheet issues from a slot, where its thickness increases or decreases because of the loss of viscous traction at the slot walls (Clarke 1968; Tillet 1968; Ruschak 1980; Georgiou, Papanastasiou & Wilkes 1988). Thus, the appropriate value of the initial exit velocity is an issue and would seemingly limit the usefulness of the equations.

Despite their limitations, the equations of Lance & Perry (1953) have been successfully used to predict the convergence length of annular water sheets exiting a vertical annular nozzle and falling under the influence of gravity (Hoffman, Takahashi & Monson 1980). It is important to note that the agreement between experiment and theory is obtained by using the average velocity at the exit of the annular nozzle without correcting for entrance region effects. The latter assumption is reasonable in the light of the work by Brown (1961), who measured the velocity in a two-dimensional liquid sheet issuing from a slot and falling vertically under the influence of gravity (hereafter called a curtain). Brown empirically obtained the following modified free-fall equation which includes the effect of viscosity:

$$V = [V_0^2 + 2g(x - 0.5(\mu/\rho)^{\frac{2}{3}})]^{\frac{1}{2}}, \tag{1}$$

where V is the fluid velocity, V_0 is the average velocity at the slot exit, g is the gravitational constant, x is the vertical distance below the slot, μ is the liquid viscosity, and ρ is the density. In (1), all units are c.g.s. Equation (1) indicates that the liquid in a curtain of low viscosity is essentially in free fall, as is the case for water.

As far as the stability of liquid sheets is concerned, Taylor (1959) has shown that a water bell can form provided that the Weber number, defined as $We = \rho d V^2/2\sigma$, is greater than one everywhere in the bell, where σ is the surface tension, d is the local thickness of the liquid sheet (which is, through a mass balance, related to the volumetric flow rate, q, by $d = q/2\pi r V$, where r is the local radial position on the axisymmetric bell), and V is given by (1) with $\mu = 0$. For the case in which gravitational effects are negligible, Taylor showed that the water bell collapses into a horizontal circular sheet with a stationary edge at the radius where $We = 1$, and thus a complete water bell is not formed. At this stationary edge, the sheet disintegrates into droplets. When gravity is important, Dumbleton (1969) showed theoretically that the bell collapses into a cone with a stationary edge at a location where $We = 1$ if the initial velocity has a component opposite to gravity. Again, the cone will disintegrate into droplets beyond this critical radius, although Taylor (1959) showed that where thickness variations in the cone are large enough (presumably to violate the

assumptions used to derive water bell equations) the critical Weber number for cone formation is smaller than 1. It should be noted that the stationary edges where $We = 1$ correspond precisely to the largest radial location where antisymmetric travelling waves can remain stationary with respect to the local fluid flow (Taylor 1959).

Despite the apparent stability implications of these water bell results, Baird & Davidson (1962) experimentally observed stable annular jets, subjected to an applied pressure, in which $We < 1$ locations were found. Baird & Davidson's descriptions of jet shapes were only qualitative, but indicated that there was a marked change in shape according to whether $We > 1$ or $We < 1$ at the annular slit from which the jet issued. Those jets for which $We > 1$ at the annular slit appeared to exit the slit vertically, and were described as being cylindrical in shape. Those jets for which $We < 1$ at the annular slit appeared to exit the slit in a direction other than vertical, and were described as being rounded. It should be noted that Baird & Davidson's explanation for this shape change is incorrect since they argue the curvature of the jet at the annular slit must change its sign as the jet makes the transition from $We > 1$ to $We < 1$, while the jet shapes they present show no such sign change.

The $We > 1$ criterion for a stable water bell has been shown to be valid for thin two-dimensional liquid curtains (Brown 1961; Lin 1981; Lin & Roberts 1981) issuing from a slot and falling vertically under the influence of gravity. In this case, We is defined as for water bells with the local curtain thickness redefined as $d = Q/V$, where Q is the volumetric flow per width of the curtain, and V is given by (1). If $We < 1$ anywhere in the falling curtain, spatially growing antisymmetric waves can exist, while if $We > 1$ everywhere in the curtain, waves formed due to disturbances decay as they are washed downstream. Thus, curtains are prone to disintegration at locations where $We < 1$, although both Brown (1961) and Lin (1981) reported cases where the curtain remained intact when $We < 1$ near the exit of the die slot. Lin & Roberts (1981) show that standing waves can be induced by placing an obstacle in the curtain. The phase lines for these antisymmetric waves are only slightly curved (due to the slowly varying thickness of the curtain) and essentially define two straight lines which intersect the obstacle at an angle which depends on the Weber number. Since viscosity plays a higher-order role in the wave speeds that are associated with the antisymmetric waves, these phase lines are identical to those shown by Taylor (1959) in his examination of waves on a horizontal inviscid liquid sheet when the effect of the slowly varying curtain thickness is neglected. If a standing wave can be produced in a curtain such that the standing wave stretches horizontally across the curtain width, then $We = 1$ at that point in the curtain, and so the curtain would be prone to disintegrate.

Despite the fact that a very small pressure difference can radically change the shape of water bells and annular jets, the effect on shape of a pressure difference across a two-dimensional curtain has not been investigated in previous work. Such a study is the focus of the present paper, which is both theoretical and experimental in nature. A set of equations is obtained in §2 whose derivation is analogous to that of water bells (Lance & Perry 1953). These equations indicate the presence of a singularity when the local Weber number equals 1 in the curtain, and a pressure difference is applied. This would not be expected to be a problem, since the previously cited literature indicates that a curtain is unstable if $We < 1$ anywhere in the curtain; thus, a curtain with this singularity would not likely form. However, our experimental results show that for a wide range of flow conditions (including those cases where there is no applied pressure), practically stable curtains can exist for $We < 1$. Thus, the derived governing equations do have a singularity which cannot be ignored. The question then arises as

to how the curtain can pass through the point where $We = 1$ when a pressure is applied.

Experimental results presented in §4 indicate that if $We < 1$ at a position in the curtain and a pressure difference is applied, the curtain will adopt a shape such that the $We = 1$ singularity is removed in the governing equations. Theoretically, the singularity can be eliminated if the curtain assumes a certain slope at the singularity location. Removal of the singularity in this way dictates that the *centreline of the curtain has a specific, non-zero slope as it leaves the die slot.* This is in marked contrast to the case where $We > 1$ everywhere in the curtain and a pressure difference is applied. Here the fluid issues from the slot in a manner such that the *centreline of the curtain has a zero slope as it leaves the die slot.* In addition, it is found that, for $We > 1$, it is not possible to determine the slope at the curtain centreline directly from our equations; thus, one must rely on either a local theoretical analysis in the vicinity of the slot or experimental results to close the problem. In this paper, the latter approach is chosen. Whether $We > 1$ or $We < 1$, our theoretical predictions of curtain shapes are in agreement with those measured experimentally. Our discussion, given in § 5, focuses on the implications of these results. Particular attention is given to the question of curtain stability for $We < 1$, as well as the implications of the above results for the number of boundary conditions that are consistent with our governing equations. Finally, we account for the previously cited observations of Baird & Davidson (1962) for an annular jet, and support this discussion with theory presented in an appendix.

2. Theory

We consider a liquid curtain issuing from a slot as shown in figure 1. For the purpose of obtaining a prediction of the curtain shape, we assume that the thickness of the curtain, h, varies very slowly as it falls vertically from the die slot. We neglect the role that viscosity plays on the dynamics of the liquid curtain, as well as the shear stress on the surface of the curtain by the friction of the air. The flow is thus locally of plug type at each streamwise location. Under these assumptions, an overall balance of forces on a differential element of the curtain, $h\,\mathrm{d}s$, yields

$$\frac{\mathrm{d}(\rho Q V)}{\mathrm{d}s}\hat{s} = (P_1 - P_2)\hat{n} + 2\sigma\left(\frac{\mathrm{d}\hat{s}}{\mathrm{d}s}\right) + \rho g h \hat{x}, \tag{2a}$$

where ρ is the liquid density, V is the velocity in the streamwise direction $\hat{s}$, Q is the volumetric flow rate per unit width, P_1 and P_2 are the pressures on the sides of the curtain, and s is the distance measured along the curtain (figure 1). Conservation of mass on the differential curtain element yields

$$Vh = V_0 h_0 = Q, \tag{2b}$$

where h_0 and V_0 are the thickness of the curtain and the average velocity at the die slot, respectively.

Equations (2) are now simplified. Using

$$\frac{\mathrm{d}\hat{s}}{\mathrm{d}s} = \frac{\mathrm{d}\theta}{\mathrm{d}s}\hat{n} \tag{3a}$$

and

$$\hat{x} = \frac{\mathrm{d}x}{\mathrm{d}s}\hat{s} - \frac{\mathrm{d}f}{\mathrm{d}x}\frac{\mathrm{d}x}{\mathrm{d}s}\hat{n}, \tag{3b}$$

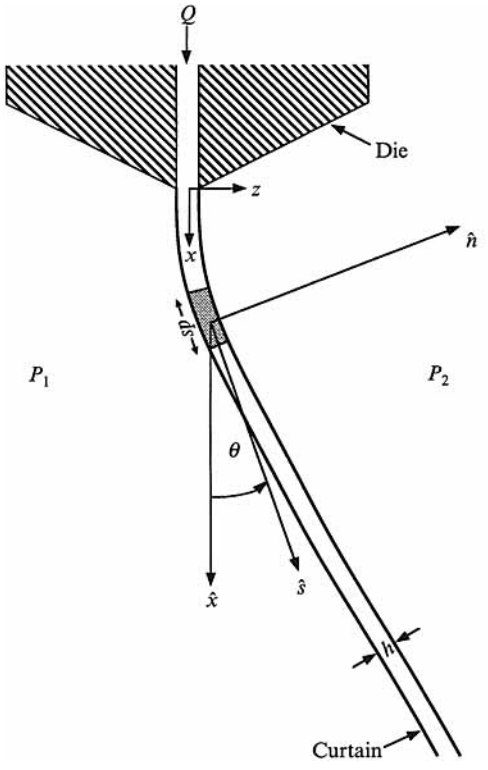

FIGURE 1. Geometry of two-dimensional curtain issuing from a slot.

the following results from the separation of (2*a*) into normal and tangential components:

$$\hat{n}\text{:}\quad (\rho QV-2\sigma)\left(\frac{\mathrm{d}\theta}{\mathrm{d}s}\right)=(P_1-P_2)-\rho gh\left(\frac{\mathrm{d}f}{\mathrm{d}x}\right)\left(\frac{\mathrm{d}x}{\mathrm{d}s}\right), \tag{4a}$$

and

$$\hat{s}\text{:}\quad \frac{\mathrm{d}(\rho QV)}{\mathrm{d}x}=\rho gh. \tag{4b}$$

In (3) and (4), $z=f(x)$ is the parameterization of the curtain location, and θ is the angle that the tangent to the curtain forms with the x-axis.

The velocity of the curtain as a function of vertical distance is obtained by substituting (2*b*) into (4*b*), rearranging and integrating from the slot exit:

$$V=(V_0^2+2gx)^{\frac{1}{2}}. \tag{5}$$

The equation for the normal component of momentum can be further simplified by substituting the expression for ρgh in (4*b*) into (4*a*) and employing the following relationship between the curvature, $\mathrm{d}\theta/\mathrm{d}s$, and f:

$$\frac{\mathrm{d}\theta}{\mathrm{d}s}=\frac{\mathrm{d}}{\mathrm{d}x}\left[\frac{\mathrm{d}f}{\mathrm{d}x}\frac{\mathrm{d}x}{\mathrm{d}s}\right], \tag{6a}$$

where

$$\frac{\mathrm{d}x}{\mathrm{d}s}=\frac{1}{[1+(\mathrm{d}f/\mathrm{d}x)^2]^{\frac{1}{2}}}. \tag{6b}$$

The simplified normal component becomes

$$\frac{\mathrm{d}}{\mathrm{d}x}\left\{\left(\frac{\mathrm{d}f/\mathrm{d}x}{[1+(\mathrm{d}f/\mathrm{d}x)^2]^{\frac{1}{2}}}\right)(\rho QV-2\sigma)\right\}=(P_1-P_2). \tag{7}$$

At this point, (7) can be integrated for any prescribed pressure distribution; however, for the purpose of this paper will assume that the pressure drop across the curtain is a constant. Using the velocity scale

$$V_s \equiv 2\sigma/\rho Q, \tag{8a}$$

we define the following dimensionless variables:

$$\bar{f}=\frac{f}{V_s^2/2g}; \quad \bar{x}=\frac{x}{V_s^2/2g}; \quad We=\frac{V}{V_s}. \tag{8b}$$

In (8) we have denoted the dimensionless velocity as We, which is the local Weber number of the curtain. Integrating (7) and employing (8), the following dimensionless equation is obtained:

$$\frac{\mathrm{d}\bar{f}/\mathrm{d}\bar{x}}{[1+(\mathrm{d}\bar{f}/\mathrm{d}\bar{x})^2]^{\frac{1}{2}}}=\frac{\alpha\bar{x}+C}{We-1}, \tag{9a}$$

where

$$We=(We_0^2+\bar{x})^{\frac{1}{2}}, \tag{9b}$$

and the slot Weber number, We_0, and pressure parameter, α, are defined as

$$We_0 \equiv \frac{V_0}{V_s}=\frac{\rho QV_0}{2\sigma}, \tag{9c}$$

$$\alpha \equiv \frac{(P_1-P_2)\,\sigma}{\rho^2Q^2g}. \tag{9d}$$

In (9a), C is a constant of integration.

It is useful to consider (9) in some detail. If inertial forces are greater than the surface tension forces everywhere in the curtain, then the solution of (9) is straightforward given a value for C. However, this is not the case when the surface tension forces are greater than the inertial forces at the slot exit, that is, $We_0 < 1$. Because the fluid in the curtain accelerates under the influence of gravity according to (9b), there is a position in the curtain, denoted by $\bar{x}_s$ where the local Weber number, We, is equal to one. Thus, a singularity arises, where the slope $\mathrm{d}\bar{f}/\mathrm{d}\bar{x}$ in (9a) is infinite. The location of this singularity is determined from (9b):

$$\bar{x}_s = 1-We_0^2. \tag{10}$$

The origin of this singularity can be seen more clearly in (4a). For the sake of discussion, let us assume that the right-hand side of (4a) is positive. Then, a surface-tension-dominated curtain, where $2\sigma > \rho QV$, would require that the curvature, $\mathrm{d}\theta/\mathrm{d}s$, be negative so that the curtain's concavity is opposite to that shown in figure 1. However, an inertia-dominated curtain, where $\rho QV > 2\sigma$, would require a positive curvature, and the curtain concavity is as shown in figure 1. Thus, the location of the singularity is that point in the curtain where the curvature requirements of surface tension and inertia precisely cancel. Equation (9a) would seem to indicate that the curtain cannot support an applied pressure at the location given by (10).

Experiments presented in §4 show that the curtain maintains a reasonable shape and can pass through the singular point intact. This leads us to consider the properties of the singularity in more detail. To this end, we expand the numerator and denominator of (9*a*) about the location of the singularity. Denoting $\bar{X} = \bar{x} - \bar{x}_s$ we write

$$\alpha\bar{x} = \alpha(\bar{X} + \bar{x}_s) \tag{11a}$$

and

$$We - 1 \sim \tfrac{1}{2}\bar{X} + O(\bar{X}^2). \tag{11b}$$

Thus, in the vicinity of the singularity, (9*a*) becomes

$$\frac{\mathrm{d}\bar{f}/\mathrm{d}\bar{x}}{[1+(\mathrm{d}\bar{f}/\mathrm{d}\bar{x})^2]^{\frac{1}{2}}} = \frac{\alpha(\bar{X}+\bar{x}_s)+C}{\frac{1}{2}\bar{X}+O(\bar{X}^2)}. \tag{12}$$

By choosing

$$C = -\alpha\bar{x}_s, \tag{13}$$

the numerator and denominator go to zero at the same rate. With such a choice of C, the slope of the curtain at the location $\bar{x} = \bar{x}_s$ is finite. A referee pointed out that (13) is consistent with the requirement that the curvature in (4*a*) be finite at the singularity location (i.e. the left-hand side of (4*a*) is zero), since the slope of the curtain at the singularity location can be determined by explicitly solving for $\mathrm{d}f/\mathrm{d}x$ on the right-hand side of (4*a*).

Note that a non-zero value of C implies that the slope of the curtain at the slot exit ($\bar{x} = 0$) is non-zero. This slope can be expressed in terms of the angle at which the fluid leaves the slot, denoted as θ_0 (i.e. the angle θ shown in figure 1 at $\bar{x} = 0$), as

$$\sin\theta_0 = \alpha(1 + We_0). \tag{14}$$

Throughout this paper for the purposes of reference, we will refer to the $We = 1$ location in the curtain as the singular point, despite the fact that the singularity is removable.

Substituting (9*b*) and (13) into (9*a*) and rearranging, we obtain the final equation that governs the shape of the curtain:

$$\frac{\mathrm{d}\bar{f}}{\mathrm{d}\bar{x}} = \frac{\alpha(1+(We_0^2+\bar{x})^{\frac{1}{2}})}{[1-\alpha^2(1+(We_0^2+\bar{x})^{\frac{1}{2}})^2]^{\frac{1}{2}}}, \tag{15a}$$

with the boundary condition at the slot exit,

$$\bar{f}|_{\bar{x}=0} = 0. \tag{15b}$$

The system (15) was derived for situations where $We_0 < 1$ at the slot exit. If fluid issues from the slot such that $We_0 > 1$, then the appropriate problem to solve for the curtain shape is given by (9), subject to boundary condition (15*b*). For this case, the integration constant in (9*a*), C, which determines the slope at the slot exit, cannot be determined with the present theory. In this paper, this constant is determined experimentally, although it is acknowledged that a local theoretical analysis in the vicinity of the slot would also allow the evaluation of C.

3. Experimental

Experiments were designed to measure the position of the planar curtain for various flow conditions and applied pressures. To this end, the liquid curtain was surrounded on all four sides by an airtight enclosure made of clear acrylic sheet, which minimized

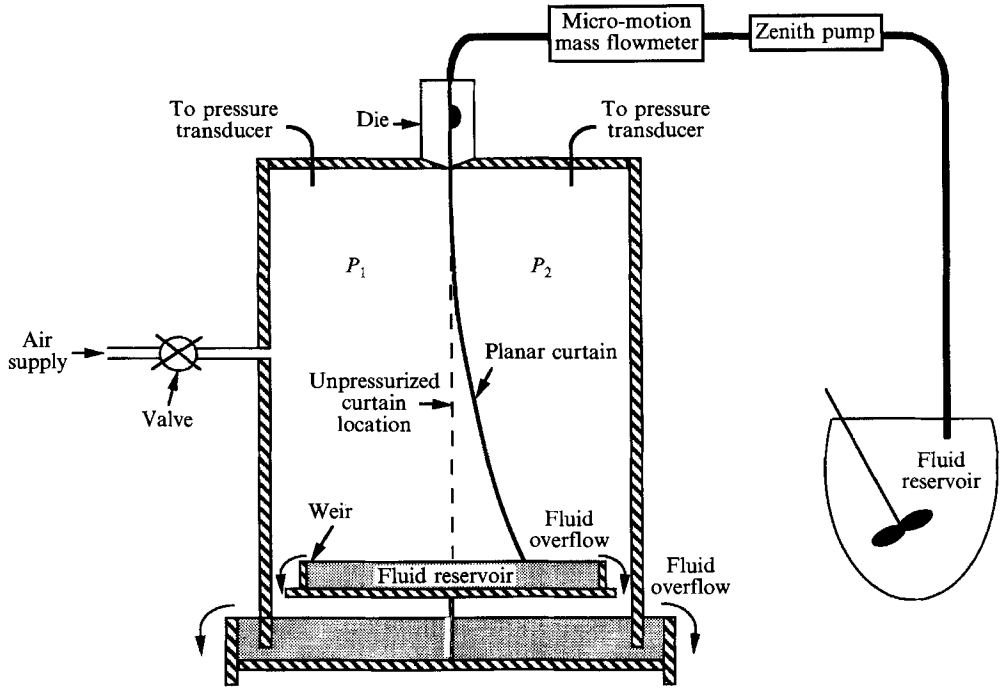

FIGURE 2. Schematic of experimental apparatus.

the effect of room pressure fluctuations on the curtain and enabled one side of the curtain to be pressurized. A schematic of the experimental set-up is shown in figure 2. The front wall of the enclosure was removable for easy access to the inside of the enclosure during curtain formation. To minimize the effects of the edges on the experiments, a curtain 20.3 cm wide and 30.5 cm high was used in all the experiments. Since the position of the curtain from vertical varied greatly throughout the experiments, the sides of the enclosure were used as the lateral supports for the curtain as it fell through the air instead of the guide wires used by Lin & Roberts (1981).

A solution of 0.5% Natrosol and water at 40 °C having a viscosity of 15 c.p.s. and a density of 1.03 g/cm^3 was used in all the experiments. Enough surfactant was added to ensure that the dynamic surface tension in the curtain was equal to the static surface tension value. The solution was delivered to the die using a Zenith metering pump and the flow rate was monitored using a MicroMotion mass flowmeter; the surface tension was determined by the overflow method (Padday 1957). The solution was evenly distributed across the width of the curtain by the use of a die with a large internal cavity and a narrow exit slot. Dies having 0.025 cm and 0.05 cm exit slot heights were used in the experiments as a means of adjusting the ratio of the volumetric flow rate to the average velocity exiting the slot.

The pressure differences used in the study were extremely small (less than 10 dynes/cm^2). Therefore, extra precautions were taken to ensure the accuracy of the pressure measurements. Two Airdata Electronic Micromanometers (Model ADM-860, accurate to ± 0.25 dynes/cm^2), one calibrated in the Kodak Corporate Standards Laboratory and the other calibrated by Shortridge Instruments using equipment traceable to the National Institute of Standards and Technology, were used to measure the pressure difference across the curtain. The two micromanometers were used simultaneously during the experiments as a guard against instrument failure. In

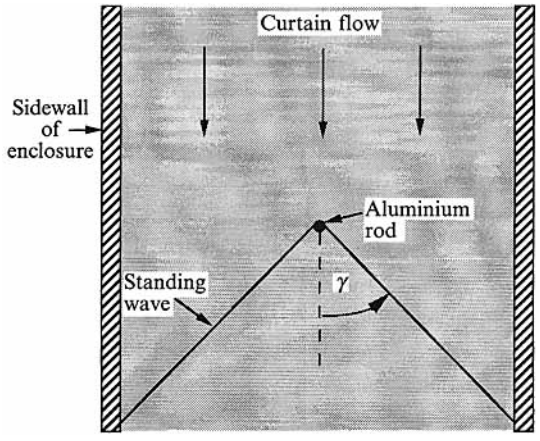

FIGURE 3. Standing waves created by a rod in the curtain (front view of curtain).

addition, the front and back sections of the enclosure were periodically opened to the atmosphere and the sensors checked for zero reading.

Extreme care was taken to form the curtains used in the experiments and to prevent them from disintegrating. The corners where the edges of the curtain met the floor of the enclosure were found to have a very large effect on the overall stability of the curtain. After much trial and error, it was found that the creation of a shallow pool of liquid at the bottom of the enclosure provided the greatest amount of stability to the curtain. In addition, the sidewalls of the enclosure were flushed with a hot water solution during the initial formation of the curtain as a means of increasing the wettability of the walls. This hot water solution was also used to prevent breakup of the curtain at the edges whenever the position of the curtain changed as it responded to increases or decreases in the applied pressure.

To measure the shape of the curtain at each condition, we electronically recorded an image of the side of the curtain through the acrylic sheet sidewall using a solid-state CCD camera. A light was used to highlight the wetting line of the side of the curtain, as well as some horizontal and vertical grooves that had been cut into the side of the acrylic sheet wall at 2.5 cm intervals for measurements purposes. The position of the curtain was then obtained by viewing and enhancing the image on a SUN workstation and using a software digitizer to find the location of the curtain as a function of vertical distance from the die slot. A check on the data was then carried out by comparing the digitized results with the known locations of the grooves in the original images.

The singular point in the curtain was experimentally determined by observing the standing waves generated by an aluminium rod of 3 mm diameter placed through the curtain (figure 3). As reported by Lin & Roberts (1981), an obstacle creates waves which intersect at a characteristic angle, γ, where γ is given by $\sin\gamma = (We)^{-\frac{1}{2}}$. Since the Weber number is equal to one at the point of singularity in the curtain, an obstacle placed at that location will have standing waves extending horizontally across the curtain (i.e. $\gamma = 90°$ in figure 3). Thus, by carefully placing the rod into the curtain, the location of the singularity in the curtain can be determined by moving the rod vertically through the curtain until the standing waves are horizontal. We found that the best way to introduce the rod into the curtain was to place it in the shallow pool at the bottom of the curtain and slowly move the rod up the curtain till the point of singularity was reached. Because the waves were difficult to see near the singular point, the accuracy of this method is limited to approximately ± 0.5 cm. In addition, when the

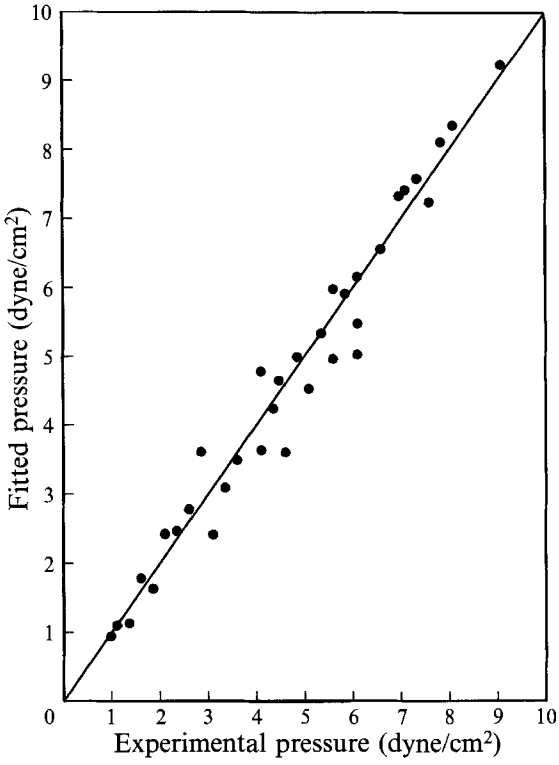

FIGURE 4. Comparison of fitted and measured pressure drops for the range of experimental $We_0 > 1$ conditions: $\sigma = 31.2$ dyne/cm, $1.3 \leqslant Q \leqslant 1.75$ cm²/s, $h_0 = 0.0254$, 0.0508 cm.

singularity was located within 3 cm of the exit of the die, it was not possible to determine the location of the singularity with any certainty since the standing waves would become lost in their reflections off the sidewalls and the die slot. Nevertheless, the observation of standing waves was sufficient to ascertain the presence or absence of a singularity in the curtain for all the flow conditions studied.

4. Results

We begin this section with some comments about curtain stability and the observed standing waves induced to form in the curtain. To within the ± 0.5 cm accuracy of locating the horizontal wave front characterizing the $We = 1$ location, the theoretical prediction of the singularity location, given by (10), was always in agreement with the experimentally observed location. Practically stable curtains were obtained for slot Weber numbers ranging from 0.02 to 2.0. The stability of the curtain was observed to degrade as the slot Weber number decreased. At the lowest slot Weber numbers, extra care had to be taken during the determination of the singularity location so as not to create a hole or free edge that would cause the curtain to disintegrate.

Examination of the CCD images of the side of the curtain showed that whenever $We_0 > 1$ the fluid excited the die parallel to the walls of the slot, that is $\mathrm{d}f/\mathrm{d}x = 0$. This finding dictates that the constant C in (9a) is equal to zero whenever $We_0 > 1$. Therefore, the shape and displacement of the curtain are determined by the $We_0 > 1$ set of equations ((9) and (15b)). To test the validity of the model, the above set of

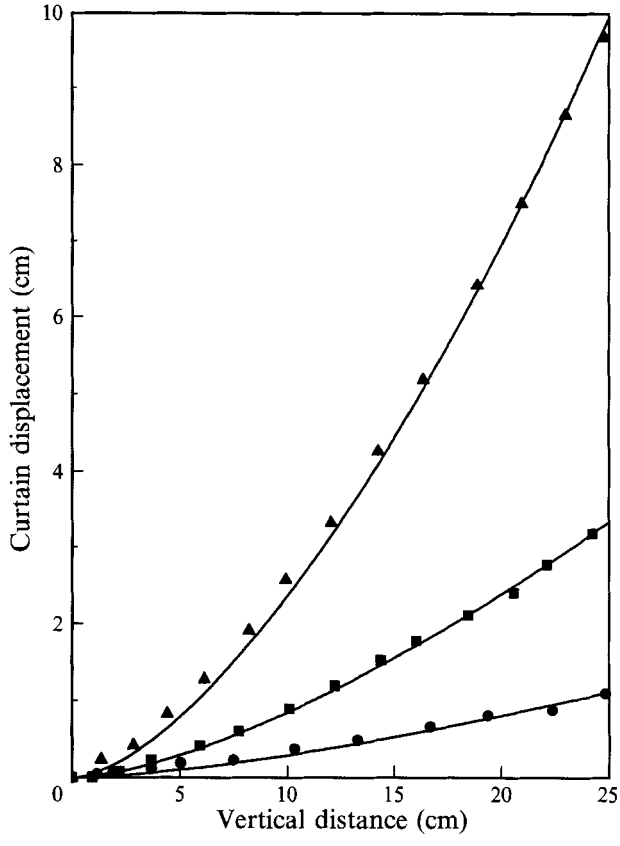

FIGURE 5. Comparison of experimental and theoretical curtain shapes for $We_0 > 1$. Theoretical predictions are solid curves obtained using fitted pressure drop, $\Delta P = (P_1 - P_2)$, for $\sigma = 31.2$ dyne/cm, $Q = 1.75$ cm^2/s, and $h_0 = 0.0254$ cm. Plot symbols are experimental measurements: ●, $\Delta P = 0.9$ dyne/cm^2; ■, $\Delta P = 2.8$ dyne/cm^2; ▲, $\Delta P = 7.6$ dyne/cm^2.

equations was solved for the curtain's location using finite differences and compared to the experimental data. Since thin liquid curtains respond readily to very low levels of applied pressure, this comparison was made by employing a nonlinear least-squares algorithm to determine the pressure that gave the best fit to the experimental curtain location data. Then, a comparison between the experimentally measured pressure and the fitted pressure was made.

For cases where $We_0 > 1$, fitted pressures are compared to the experimental values in figure 4, where pressures ranged from 0.9 to 9.1 dynes/cm^2. The solid line in figure 4 is the line of perfect agreement between the experimental and the fitted theoretical pressures. The scatter in the figure can partially be accounted for by the ± 25 dyne/cm^2 measurement precision of the micromanometers. We cannot specifically account for the additional error contributions to the scatter in figure 4, although the assembly of the apparatus itself contributed, and it is also possible that air flows due to the fluid motion in the curtain caused the local pressure to be different from the measured pressure. Regardless of the additional sources of scatter, we note that the pressure error was non-systematic. Figure 5 shows the curtain shape measurements for three different applied pressures for the situation where $We_0 > 1$. Included in the figure is the theoretically predicted shape using the fitted pressure. The experimental data are seen to agree with the predicted curtain position over the entire length of the falling curtain.

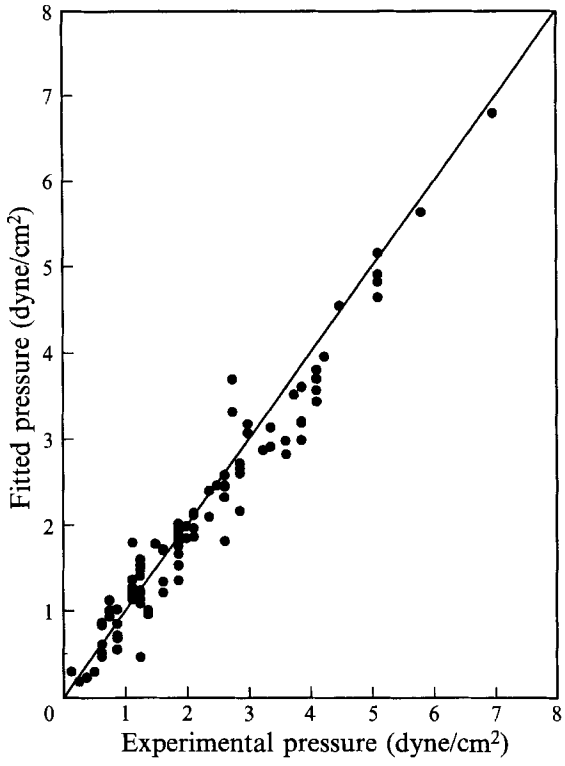

FIGURE 6. Comparison of fitted and measured pressure drops for the range of experimental $We_0 < 1$ conditions: $\sigma = 31.2$, 50 dyne/cm, $0.26 \leqslant Q \leqslant 1.65$ cm²/s, $h_0 = 0.0254$, 0.0508 cm.

This, coupled with the pressure data in figure 4, indicates that the theory and experiments agree. Note that even at the highest applied pressure the solution exits the slot with a zero slope.

Curtains having $We_0 < 1$ were also studied. Using the procedure previously described, fitted pressure values were obtained using the finite-difference solution to (15*a*) and (15*b*). The fitted pressure results are compared to the experimentally measured values in figure 6, where pressures ranged from 0.125 to 7.1 dynes/cm². As for the $We_0 > 1$ case, there is a similar non-systematic pressure error seen over the entire range of applied pressure. A comparison between the experimental and fitted curtain shapes for three applied pressures is shown in figure 7. The results of figures 6 and 7 indicate that there is agreement between the experiment and theory. It is clear from figure 7 that the liquid exits the die slot with a non-zero slope. Unlike the results when $We_0 > 1$, the slope of the curtain at the exit increases as the applied pressure increases.

The initial velocity used in the theoretical calculations was the total flow rate per unit width divided by the height of the die slot. However, it is known that the curtain can increase or decrease in thickness as it leaves the die depending upon the flow conditions (Clarke 1968; Tillet 1968; Ruschak 1980; Georgiou 1988). Therefore, a study was performed to determine the sensitivity of the fitted pressure to the value of the initial velocity. Two flow conditions corresponding to the maximum and minimum applied pressures used in the study were checked. It was found that, even when the initial velocity was allowed to vary by $\pm 25\%$ of the nominal value, the resultant pressure varied by no more than 6% from the value obtained using the nominal initial velocity.

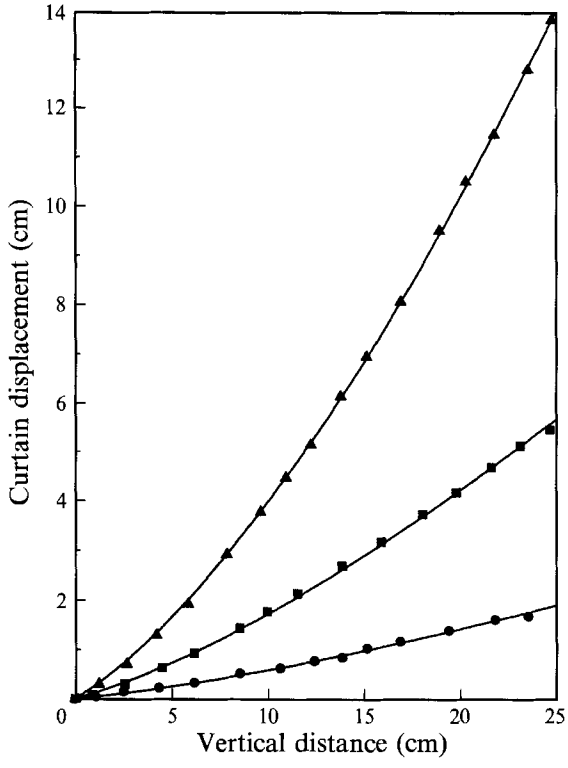

FIGURE 7. Comparison of experimental and theoretical curtain shapes for $We_0 < 1$. Theoretical predictions are solid curves obtained using fitted pressure drop, $\Delta P = (P_1 - P_2)$, for $\sigma = 31.2$ dyne/cm, $Q = 0.87$ cm^2/s, and $h_0 = 0.0254$. Plot symbols are experimental measurements: ●, $\Delta P = 0.6$ dyne/cm^2; ■, $\Delta P = 1.8$ dyne/cm^2; ▲, $\Delta P = 3.8$ dyne/cm^2.

These results support our assumption that the rearrangement of the flow in the region of the slot exit (due to the loss of the no-slip condition at the walls) does not have a large effect on the predicted slope of the curtain at the die exit.

Thus far, we have considered curtain shapes for cases where there is a singularity in the curtain, or where there is no singularity in the curtain and $We > 1$ everywhere (i.e. the singularity lies below). For these cases, a pressure drop across the curtain will cause the curtain to curve in the direction of the lower pressure (see figures 8*a* and 8*b*). A natural question to consider is what happens when there is no singularity in the curtain and $We < 1$ everywhere (i.e. according to (10) the singularity would lie below the location where the curtain impinges on the fluid reservoir shown in figure 2 if the curtain were fictitiously extended). Our experiments showed that the curtain radically changes its shape for this case. In particular, for a pressure drop across the curtain, the curtain curves in the direction of the higher pressure (figure 8*c*). Thus, the sense of the curvature is as would be expected for a bubble having surface tension.

Cases where $We < 1$ everywhere and there was no singularity in the curtain exhibited an extreme sensitivity to the applied pressure; very small pressure drops led to large differences in curtain location. Thus, pressure drop measurements were not reliable for this flow regime. Furthermore, we found that the impingement point in the liquid reservoir, as well as the angle at which the curtain left the slot, was extremely sensitive to the way in which the curtain pinned to the wall. It was thus not possible to compare accurately experiments and theory for these cases. Nevertheless, it is clear that when

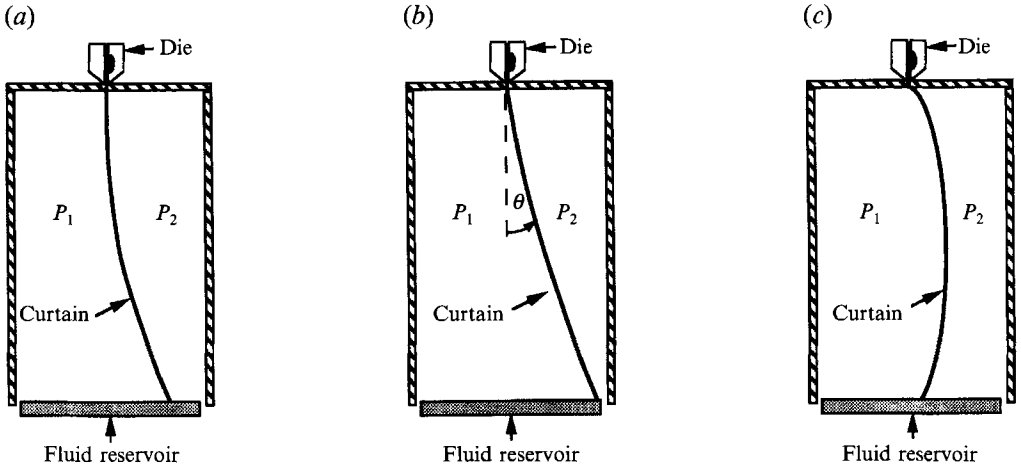

FIGURE 8. Curtain shapes for various singularity locations, where $P_1 > P_2$. (*a*) Singularity lies above the curtain, $We_0 > 1$; the curtain issues parallel to the walls of the die slot. (*b*) Singularity lies in the curtain, $We_0 < 1$; the curtain issues at an angle θ from the die slot. (*c*) Singularity lies below the bottom of the curtain, $We_0 < 1$.

$We < 1$ everywhere and there is no singularity in the curtain, our governing equations (9) do predict that the sense of the curvature will be as that shown in figure 8(*c*). Furthermore, the angle or position associated with the impingement of the curtain into the fluid reservoir determines the constant C in (9); it thus has a large effect on the curtain shape. As in the case where $We > 1$ everywhere, the constant C is not determined by the present theory.

5. Discussion

We begin this section by examining the structure of the equations for $We < 1$ and $We > 1$ in the context of wave motion. The Weber number itself can be viewed as a ratio of the local fluid velocity, V, to that of antisymmetric waves travelling both upstream and downstream at velocity V_s given by (8*a*) (Lin & Roberts 1981). Thus, for $We > 1$, the curtain velocity locally is greater than that of waves which travel upstream. Consequently, the curtain itself acts to convect flow information away from the slot and downstream. The governing equations (9) reflect this fact by allowing the slope at the slot exit to be arbitrary (C is undetermined) so that boundary conditions can be stacked at one end of the domain (at the slot exit). Our experiments support this since $C = 0$ allows experimentally confirmed predictions of curtain shapes over a wide range of flow conditions where $We > 1$; thus, conditions at the downstream end of the curtain are not influencing its shape.

However, for cases where there are $We < 1$ locations in the curtain, the wave velocity travelling upstream is greater than that of the local curtain velocity. Consequently, the downstream locations of the curtain where $We < 1$ can influence the upstream curtain shape. From this point of view, the elimination of the singularity, which determines the constant C in (9), can be viewed as equivalent to a downstream boundary condition. Such a downstream boundary condition implies that the slope of the curtain at the slot exit is non-zero. On the other hand, with respect to the rest of the curtain where $We > 1$, the curtain location and slope just beyond the singularity could be viewed as boundary conditions that only affect the curtain downstream. If the Weber number is

decreased further such that there is no singularity in the curtain, then information at the bottom of the curtain can reach the top, and visa versa. Consequently, in (9), the governing equations reflect this fact by allowing the slope at the slot exit, characterized by C, to be arbitrary. In contrast to the case where $We > 1$, however, where C was also arbitrary, the slope at the slot exit is influenced by the boundary condition at the bottom of the curtain; as discussed in §4, our experiments showed that the location of impingement into the pool of liquid at the curtain bottom was seen to affect the slope at the slot exit. The above-described differences in structure between $We > 1$ everywhere and $We < 1$ everywhere are reminiscent of the difference between hyperbolic and elliptic linear equations, respectively, used to describe supersonic and subsonic flows.

Our results indicate both the utility and limitations in applying the derived governing equations of §2. It is clear that, as in axisymmetric geometries (Hopwood 1952; Lance & Perry 1953; Ramos 1988), the experimental curtain shapes of §4 show a large sensitivity to the pressure drop across the curtain. Thus, careful pressure measurements are required to use the equations in a predictive way. On the other hand, curtain shapes are relatively insensitive to the rearrangement of the flow (due to the loss of the no-slip condition at the slot walls) in the immediate vicinity of the slot where our equations are not valid; consequently, it suffices to use the average velocity of the fluid at the slot exit in the equations, at least when low-viscosity fluids are employed. This conclusion is supported by equation (1), which was empirically obtained by Brown (1961) for fluid falling from a slot. This same equation shows that even when viscosity is important, the viscosity effect can be incorporated into the initial velocity at the slot exit. With this change, we expect our equations to be valid also at higher viscosities, since the velocity is still free fall with a modified initial velocity.

We now comment on the stability of the curtains in our experiments. As discussed in §1, work by Brown (1961) and Lin (1981) indicate that a curtain is not stable if $We < 1$ for any location in the curtain. Both Brown (1961) and Lin & Roberts (1981) do report that curtains can still exist if the local Weber number is less than 1, provided that the location where $We = 1$ is in the vicinity of the slot. Lin & Roberts (1981) attribute this apparent stability as being due to parameter values being outside the range of validity of the linear stability analysis used to derive the $We = 1$ criteria. However, our experiments show that practically stable curtains can exist over a broad range of conditions where $We < 1$ locations are found *in* or *over the entire* curtain. This is despite the fact that curtains investigated in this work do satisfy the conditions of Lin's stability analysis. We argue here that the $We = 1$ criterion is based on a linear theory which does not represent the limit of practical stability. In order for the curtain to disintegrate, it is necessary for the curtain to thin to molecular dimensions and a perforation form – a free edge leads to rapid curtain disintegration. This thinning phenomenon by its nature violates the conditions of a linear stability analysis of the undisturbed curtain flow. As the curtain thins, there may be nonlinear effects which act to reduce the growth rates of the disturbances and stabilize the curtain. We employed surfactant, which clearly has a stabilizing effect (Rosen 1989) but is not essential to producing a curtain with $We < 1$. In addition, the growth rates of the long waves, upon which the stability analysis conclusions are based, are very small. These long waves grow *spatially*, and not temporally (Lin 1981); thus, growing disturbances at a given location will not amplify in time as the curtain flow continues. As long as disturbances impinging on the curtain have small amplitudes, the wave growth occurring over the length of the curtain may not be sufficient to approach a nonlinear regime in which the curtain could disintegrate.

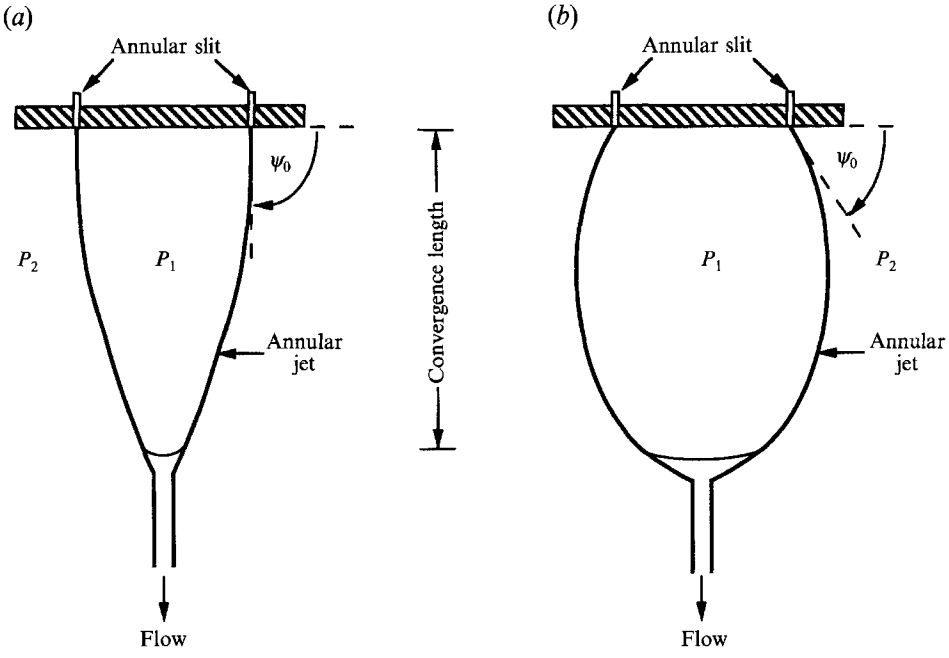

FIGURE 9. Qualitative annular jet shapes reported by Baird & Davidson (1962): (*a*) $We > 1$ at annular slit, $\psi_0 = 90°$; (*b*) $We < 1$ at annular slit, $\psi_0 < 90°$.

We close this paper by theoretically explaining the qualitative observations of Baird & Davidson (1962) for an annular jet issuing from a vertical annular slit, where there is a pressure drop across the jet. As discussed in §1, Baird & Davidson observed two classes of jet depending on the Weber number at the annular slit from which the jet issued. For $We > 1$ at the slit, they assumed that the jets issued the slot parallel to the slit walls (figure 9*a*), and their experimental measurements of convergence length of the jet were in good agreement with the theory. For $We < 1$ at the slit, there were no experimental measurements or theoretical shapes provided, but some qualitative shapes were sketched indicating there was an angle at which the jet issues from the annular slit (figure 9*b*), despite the fact that the slit was oriented vertically. Baird & Davidson (1962) incorrectly explained their observations based on a differing sign of the radius of curvature (in the vertical plane) for the two cases, while the jet shapes they present have the same curvature sign.

An explanation of the annular jet observations can be made using the mathematical approach described for the planar curtain. As shown in the Appendix, a singularity similar to the one for the planar curtain arises for the annular jet in the absence of gravitational effects, when fluid inertia supplied by the radial motion of the liquid balance the surface tension forces (compare (A 2) with (4*a*)). The mathematical elimination of the singularity leads to a specified slope at the singularity location, which yields a non-zero exit angle for the annular curtain when $We < 1$ (this angle is given by (A 6*b*)). We also note that for $We < 1$, the qualitative shape of the annular jet (in the vertical plane) reported by Baird & Davidson (1962) appears to be a section of a circular arc, which is precisely the solution obtained when the singularity is eliminated, as shown by (A 6*a*). The curvature for the $We > 1$ and $We < 1$ cases have the same sign; it is the angle at the slot that is the distinguishing feature between the two cases. Finally, we comment that in either the planar or annular geometries, it is the presence

of a pressure drop which allows the curtain to assume a non-zero slope when $We < 1$ at the location where the curtain forms, and such a slope is determined by the elimination of a singularity arising due to the opposing effects of inertia and surface tension.

Appendix. Elimination of the singularity in the axisymmetric problem

The purpose of this Appendix is to demonstrate how the singularity found in the work of Baird & Davidson (1962) can be eliminated, for the case of a jet issuing from an annular slit. We begin with equation (4) of their work which is obtained by a balance of normal forces on the axisymmetric jet (see figure 10), which is rewritten in slightly different form to reflect the different notation used:

$$2\sigma\left(\frac{\sin\psi}{r}+\frac{\mathrm{d}\psi}{\mathrm{d}s}\right)+\frac{\rho Qg\cos\psi}{2\pi rV}-\Delta P=\frac{\rho QV}{2\pi r}\frac{\mathrm{d}\psi}{\mathrm{d}s}. \tag{A 1}$$

In (A 1), ψ is defined as the angle between the jet and the horizontal plane as shown in figure 10, s is the arclength measured in the flow direction, r is the distance from the jet to the axis of symmetry, $\Delta P = (P_1 - P_2)$, where P_1 and P_2 are the pressures inside and outside the axisymmetric annular jet, respectively, and V is given by (5) of our paper. Note also that Q is defined here as the volumetric flow rate of the curtain, not as the mass flow rate as in Baird & Davidson, accounting for the explicit appearance of the density, ρ, in (A 1).

Following Baird & Davidson, we neglect gravity in (A 1) and (5), and rearrange, to yield

$$\left(2\sigma-\frac{\rho QV_0}{2\pi r}\right)\frac{\mathrm{d}\psi}{\mathrm{d}s}=\Delta P-2\sigma\frac{\sin\psi}{r} \tag{A 2}$$

which is analogous to equation (4*a*) of our paper. In (A 2), the velocity at the annular slit, V_0, is related through a mass balance to the volumetric flow rate in the curtain as $V_0 = Q/(2\pi r d_0)$, where d_0 is the gap spacing of the annular slit. At this point, we depart from Baird & Davidson, who further simplify (A 2) by assuming that the annular jet is nearly vertical, and that $\mathrm{d}\psi/\mathrm{d}s \ll 1/r$. Defining $x = f(r)$ as the parameterization of the interface shape in the vertical plane (it is seen in what follows that this particular parameterization leads to governing equations which are analogous to that for planar curtain) and identifying

$$\frac{\mathrm{d}\psi}{\mathrm{d}s}=\frac{\mathrm{d}^2f/\mathrm{d}r^2}{[1+(\mathrm{d}f/\mathrm{d}r)^2]^{\frac{3}{2}}},\quad \sin\psi=\frac{\mathrm{d}f/\mathrm{d}r}{[1+(\mathrm{d}f/\mathrm{d}r)^2]^{\frac{1}{2}}}$$

equation (A 2) can be written after rearrangement as

$$\frac{\mathrm{d}}{\mathrm{d}r}\left[\left(2\sigma r-\frac{\rho QV_0}{2\pi}\right)\frac{\mathrm{d}f/\mathrm{d}r}{[1+(\mathrm{d}f/\mathrm{d}r)^2]^{\frac{1}{2}}}\right]=\Delta Pr. \tag{A 3}$$

We now assume that the pressure drop across the jet is constant. Making both f and r dimensionless with r_0, the radius of the annular slit at $z = 0$, and integrating (A 3) once, the result is

$$\frac{\mathrm{d}\bar{f}/\mathrm{d}\bar{r}}{[1+(\mathrm{d}\bar{f}/\mathrm{d}\bar{r})^2]^{\frac{1}{2}}}=\frac{\alpha\bar{r}^2+C}{\bar{r}-We_0}, \tag{A 4a}$$

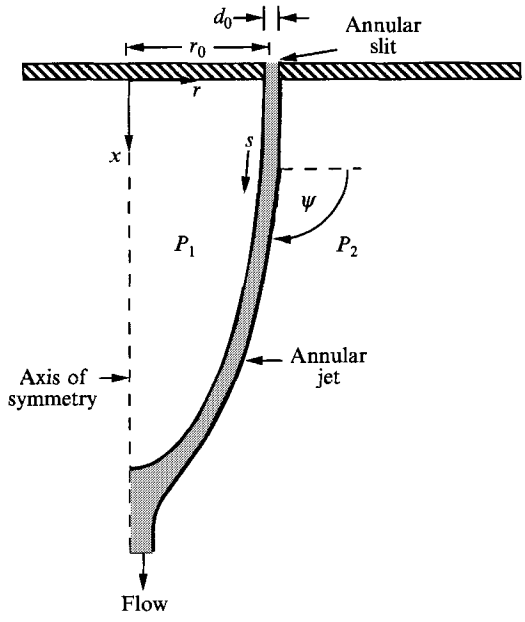

FIGURE 10. Geometry of an axisymmetric annular jet issuing from an annular slit.

where the overbars denote dimensionless quantities and C is an arbitrary constant which determines the slope of the jet leaving the slit. In (A 4a), the pressure parameter, α, and the Weber number at the slit, We_0, are defined as

$$\alpha = \frac{\Delta P r_0}{4\sigma}, \quad We_0 = \frac{\rho Q V_0}{4\pi\sigma r_0}. \tag{A 4b, c}$$

We note that We_0 in (A 4c) is precisely that defined by Baird & Davidson. For the annular jet, the following boundary condition applies at the annular slit:

$$\bar{f} = 0 \quad \text{at} \quad \bar{r} = 1. \tag{A 4d}$$

The system (A 4) is analogous to the system (9) and (14b) in our paper for the case of a planar curtain.

We now consider the solution to (A 4). If fluid exits the slot such that $We_0 > 1$, the experimental observations of Baird & Davidson indicate that the jet leaves the annular slit parallel to the slit walls, i.e. $\psi = \frac{1}{2}\pi$ at the slit in figure 10; this observation is consistent with the other annular jet literature cited in §1. For such a case, the value of the constant C in (A 4a) is given by

$$C = We_0 - 1 - \alpha.$$

This constant implies that the slope of the annular jet, i.e. $\mathrm{d}\bar{f}/\mathrm{d}\bar{r}$, increases from $-\infty$ monotonically as r increases, which is consistent with the $We_0 > 1$ shapes shown by Baird & Davidson (figure 9a).

Next, suppose that the fluid issues the slit such that $We_0 < 1$. At the slit itself, $\bar{r} = 1$, and thus if the annular jet is to converge, the denominator in (A 4a) must go through zero at the radius where $\bar{r} = We_0$. Thus, we consider the elimination of the singularity by the choice of C, as was done for the planar curtain. By choosing

$$C = -\alpha We_0^2$$

the singularity can be eliminated and (A 4*a*) becomes

$$\frac{\mathrm{d}\bar{f}/\mathrm{d}\bar{r}}{[1+(\mathrm{d}\bar{f}/\mathrm{d}\bar{r})^2]^{\frac{1}{2}}} = \alpha(\bar{r}+We_0). \tag{A 5}$$

This equation can be integrated analytically, subject to the boundary condition (A 4*d*), to yield

$$\left[\bar{f}-\left(\frac{1}{\alpha^2}-(1+We_0)^2\right)^{\frac{1}{2}}\right]^2+(\bar{r}+We_0)^2=\frac{1}{\alpha^2}, \tag{A 6a}$$

i.e. $\bar{f}$ is a circular arc of radius $1/\alpha$. Finally, we note that the angle, ψ_0, at which the curtain leaves the slit is given by

$$\sin\psi_0 = \alpha(1+We_0). \tag{A 6b}$$

Thus, it is seen that as in the planar problem, the elimination of the singularity has specified that the jet leave the annular slit with a direction other than vertical for $We_0 < 1$ (figure 9*b*).

REFERENCES

BAIRD, M. H. I. & DAVIDSON, J. F. 1962 Annular jets – I. Fluid dynamics. *Chem. Engng Sci.* **17**, 467–472.

BOUSSINESQ, J. 1869*a* Theorie des experiences de Savart sur la forme que prend une veine liquide apres s'etre heurtee contre un plan circulaire. *C. R. Acad. Sci., Paris* **69**, 45–48.

BOUSSINESQ, J. 1869*b* Theorie des experiences de Savart sur la forme que prend une veine liquide apres s'etre heurtee contre un plan circulaire. *C. R. Acad. Sci. Paris* **69**, 128–131.

BROWN, D. R. 1961 A study of the behaviour of a thin sheet of a moving liquid. *J. Fluid Mech.* **10**, 297–305.

CLARKE, N. S. 1969 Two-dimensional flow under gravity in a jet of viscous liquid. *J. Fluid Mech.* **31**, 481–500.

DUMBLETON, J. H. 1969 Effect of gravity on the shape of water bells. *J. Appl. Phys.* **40**, 3950–3954.

GEORGIOU, G. C., PAPANASTASIOU, T. C. & WILKES, J. O. 1988 Laminar Newtonian jets at high Reynolds number and high surface tension. *AIChE J.* **34**, 1559–1562.

HOFFMAN, M. A., TAKAHASHI, R. K. & MONSON, R. D. 1980 Annular liquid jet experiments. *Trans. ASME* I: *J. Fluids Engng* **102**, 344–349.

HOPWOOD, F. L. 1952 Water bells. *Proc. Phys. Soc. Lond.* B **65**, 2–5.

LANCE, G. N. & PERRY, R. L. 1953 Water bells. *Proc. Phys. Soc. Lond.* B **66**, 1067–1072.

LIN, S. P. 1981 Stability of a viscous liquid curtain. *J. Fluid Mech.* **104**, 111–118.

LIN, S. P. & ROBERTS, G. 1981 Waves in a viscous liquid curtain. *J. Fluid Mech.* **112**, 443–458.

PADDAY, J. F. 1957 A direct reading electrically operated balance for static and dynamic surface-tension measurement. *Proc. Intl Congr. of Surface Activity* (ed. J. H. Schulman), vol. 1, pp. 1–6. Academic.

RAMOS, J. I. 1988 Liquid curtains – I. Fluid mechanics. *Chem. Engng Sci.* **43**, 3171–3184.

ROSEN, M. J. 1989 *Surfactants and Interfacial Phenomena.* John Wiley & Sons.

RUSCHAK, K. J. 1980 A method for incorporating free boundaries with surface tension in finite-element fluid-flow simulators. *Intl. J. Numer. Meth. Engng* **15**, 639–648.

TAYLOR, G. I. 1959 The dynamics of thin sheets of fluid – III. Disintegration of fluid sheets. *Proc. R. Soc. Lond.* A **253**, 18–21.

TILLET, J. P. K. 1968 On the laminar flow of a free jet of liquid at high Reynolds numbers. *J. Fluid Mech.* **32**, 273–292.